

Jozef Vojtko

Technical University of Košice  
Faculty of Electrical Engineering and Informatics  
Department of Theory of Electrical Engineering and Measurement  
042 00, Slovak Republic, e-mail: Jozef.Vojtko@tuke.sk

## USING NEURAL NETWORKS FOR ERROR SUPPRESSION IN NONLINEAR SYSTEMS WITH HYSTERESIS

Some shortcomings of nonlinear systems with hysteresis are relatively big errors, e.g. linearity error, hysteresis error, etc. The paper deals with possible improvements in the methods of error suppression by using neural networks. Another aim of the paper is evaluation of measurement uncertainty. It reviews the procedures currently applied for measurement uncertainty calculation according to ISO Guide.

Keywords: measurement, sensor errors, error suppression, uncertainty, neural network

### 1. INTRODUCTION

Many systems in engineering industry are nonlinear and show hysteresis behavior. An elastomagnetic sensor is exactly the type of nonlinear system with hysteresis. It is based on the elastomagnetic phenomenon, i.e. a change of mechanical stress causes a change of magnetic properties of the ferromagnetic sensor core and it corresponds with a change of the output sensor voltage. The sensor is connected like a transformer (see Fig. 1). The sensor core is made of 50 steel sheets; the number of primary turns is 10 and number of secondary turns is 8. These parallel windings are placed in four cross-holes. A more detailed description of the sensor is in [10].

The change of magnetic properties of steel under the influence of a mechanical load [5] is analogous to the electric resistance of conductors used in strain gauges. The magnetic characteristics of amplitude permeability and incremental permeability in a properly chosen working point are about 100 times more stress-sensitive than these electrical resistance effects. The relative change of the steel magnetic incremental permeability is up to  $10^{-3}$ /MPa, whereas the relative change of a strain gauge electric resistance is about  $10^{-5}$ /MPa. The elastomagnetic method, therefore, enables the measurement of stress changes under 1MPa without problem in a noisy industrial environment and over a wide temperature range, also in cases when the use of other methods is impossible [9]. Shortcomings of elastomagnetic sensors are: ambiguity of transfer characteristic and sensor errors, e.g. linearity and hysteresis errors [12].

At present, the requirements for accuracy and reliability of sensor measuring systems are getting higher. The total accuracy of the measuring system can be significantly improved by adding a data conditioning block which can be represented by a neural network.

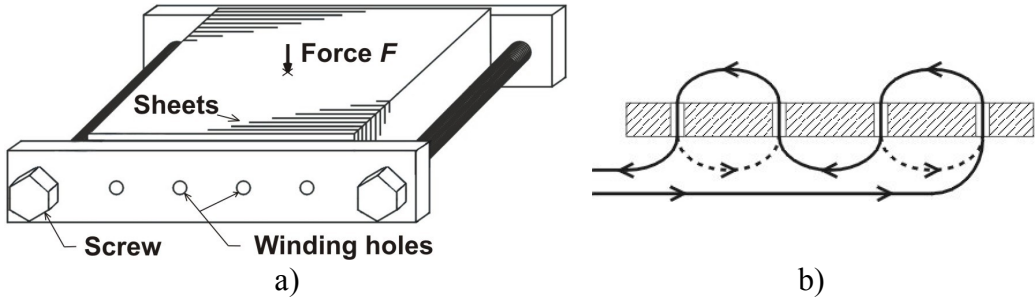


Fig. 1. Elastomagnetic sensor a) sketch of the sensor, b) winding process of sensor coils.

## 2. MEASUREMENTS

The hysteresis behavior of nonlinear systems causes an impossibility of exact conversion of an output sensor quantity into units of measurand (output sensor voltage into measured force in the case of the elastomagnetic sensor). Therefore, some methods may be used for the conversion and sensor error suppression. Using conventional methods, for example an approximation or a look-up table, can not sufficiently suppress the sensor errors. An unconventional solution can be using of neural networks for the conversion and sensor errors suppression. We suppose that the performance of neural networks is better than that of other conventional techniques for the conversion. Existing solutions which overcome the shortcomings of sensors are based on feedforward neural networks [1], [11]. However, they do not include a time-dimension and can not suppress hysteresis error of the sensor. The proposed solution uses feedforward neural networks which are extended to input. This extension represents time series of input patterns and it allows hysteresis suppression.

Let us look first at the output sensor characteristic. In accordance with the IEC 61 298-2 standard [4], the output sensor characteristic is obtained by using measuring apparatus (see Fig. 2). The optimal working parameters for sensor EMS-120kN are: feeding AC current 0.70 A, frequency 400 Hz [7]. The range of the sensor output voltage is from 1630 mV (unloaded sensor) to 930 mV (loaded sensor).

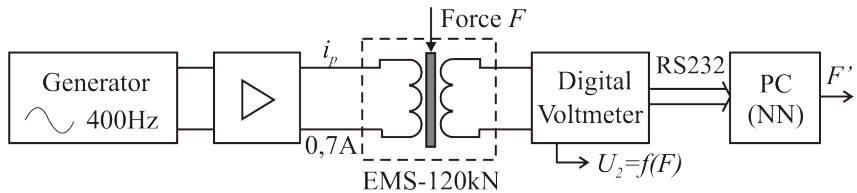


Fig. 2. Measuring apparatus.

The influence of feeding current instability has a sizeable effect on sensor accuracy. In order to eliminate it, the feeding circuit has to fulfill a basic condition - the feeding current must be constant. In this case, a change of output secondary voltage  $U_2$  will be proportional to a change of acting pressure force on the sensor core. The measured characteristics of output voltage  $U_{2\uparrow}$  (if force  $F$  is increasing from 0 kN to 120 kN) and  $U_{2\downarrow}$  (if force  $F$  is decreasing from 120 kN to 0 kN) are shown in Fig. 3.  $U_{2lin}$  is a straight line calculated by the least squares method; linear output characteristic:  $U_{2lin} = -6.0726F + 1658.21$ .

A classic approach assumes a linear static transfer characteristic. We can calculate force  $F$  corresponding to the sensor output voltage  $U_2$  (or  $F_\uparrow$  calculated from  $U_{2\uparrow}$  and  $F_\downarrow$  calculated from  $U_{2\downarrow}$ ):

$$F = -\frac{U_2 - 1658.21}{6.0726}. \quad (1)$$

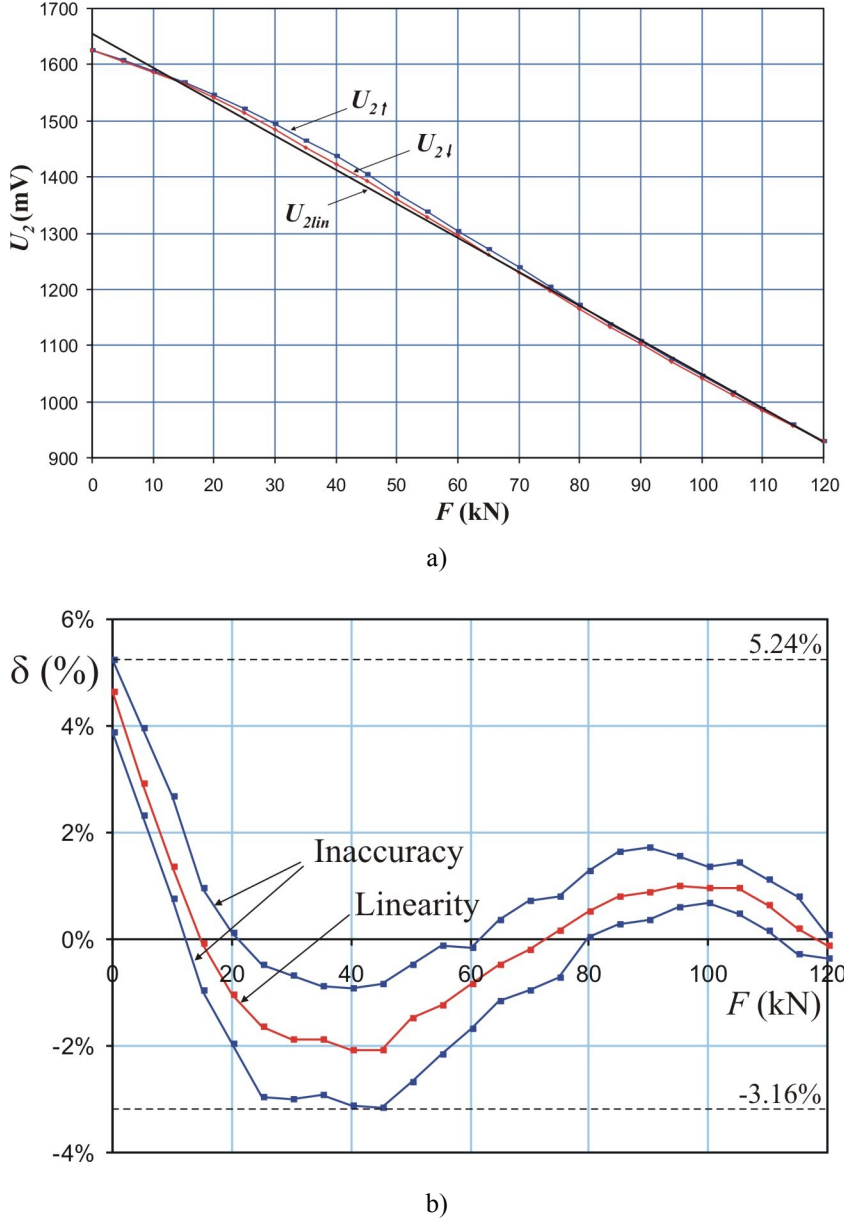


Fig. 3. Characteristics a) measured output sensor voltage ( $U_2 = f(F)$ ), b) sensor errors - inaccuracy and linearity error ( $\delta = f(F)$ ).

The standard tests are done in accordance with [3], [4]: inaccuracy, measured error, repeatability, hysteresis, and linearity error determined from five upscale and downscale full-range traverses ( $n = 5$ ), measured at twenty five points. **Inaccuracy** is a characteristic of the measurement process and describes the (lack of) accuracy. It is determined as the greatest positive and negative deviations of any measured value from the ideal value for increasing and decreasing inputs for any test cycle separately, and reported in percent of ideal output span. **Measured error** is determined as the greatest positive or negative value from the ideal value from the average upscale errors and the average downscale errors. **Repeatability** is defined as the closeness of agreement among a number of consecutive output values measuring the same input value under the same operating conditions, approaching from the

same direction. Usually measured as non-repeatability but expressed as repeatability, a percentage of span. **Hysteresis**  $\delta_{hys}$  is defined as the maximum difference in output for any given input (within the specified range) when the value is approached first with increasing and then with decreasing input signals (usually expressed as a percentage of span) (2). **Linearity error**  $\delta_{lin}$  is defined as the maximum deviation of any point from a straight line drawn as a "best fit" through the calibration points of an instrument with a linear response curve (usually expressed as a percentage of span) (3).

$$\delta_{hys} = \left\{ \frac{\sum |F'_z - F'_{\uparrow}|}{F_{max} - F_{min}} \right\}_{\check{r}_{max}}, \quad (2)$$

$$\delta_{lin} = \left\{ \frac{\sum |F'_{ave} - F|}{F_{max} - F_{min}} \right\}_{\check{r}_{max}}, \quad (3)$$

$$F'_{ave} = \frac{\sum_{i=1}^n \frac{\sum F'_{\uparrow i} + F'_{\downarrow i}}{2}}{n}, \quad (4)$$

where  $F'_{\uparrow}$ ,  $F'_{\downarrow}$ ,  $F'_{ave}$  and  $F$  are vectors with 25 elements,  $F_{max} = 120$  kN,  $F_{min} = 0$  kN.

Following previous definitions, the sensor errors are computed in Table 1.

Table 1. Sensor errors.

sensor error	label	value
Inaccuracy	$\delta_{ina}$	-3.16 %; 5.24 %
Measured error	$\delta_{me}$	4.63 %
Repeatability	$\delta_{rep}$	1.65 %
Hysteresis	$\delta_{hys}$	2.13 %
Linearity error	$\delta_{lin}$	4.63 %

The inaccuracy is the most important parameter for determination of uncertainty. It includes random and systematic errors and can be expressed by the next equation:

$$\delta_{ina} = \delta_{rep} + \delta_{me} + \delta_{hys} \quad (5)$$

### 3. PROPOSED MODEL

Feedforward neural networks can be applied as an alternative mathematical tool for universal function approximation. There is no general rule yet how to design a good neural network model, but there are many possibilities in experimental methods.

The proposed model in the paper implies that it has some special properties, known from the Preisach model as "wiping out property" (some input extreme can remove the effects of a previous extreme) and "congruent minor loop property" [8]. We can assume the existence of minor up-loops and minor down-loops inside the major one; it is shown in Fig. 4.

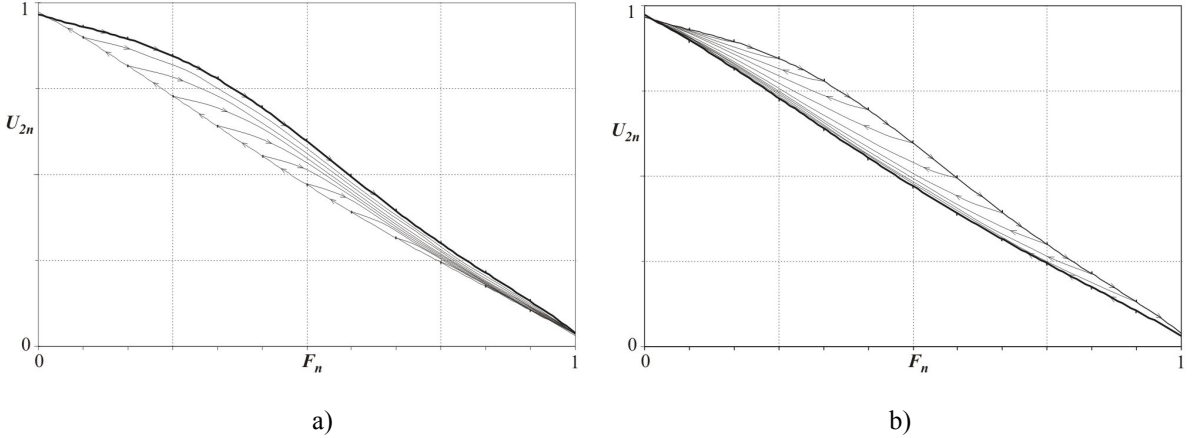


Fig. 4. Four times enlarged measured characteristics for better viewing; a) minor up-loops and b) minor down-loops.

Due to these properties, a training set can be expanded from 2 vectors with 25 measured points at upscale and downscale full-range traverses to the two matrixes with dimension (2, 350), where the first row consists of measured points and the second consists of parameter  $\zeta$ .

$$\zeta(t) = U_2(t) - U_2(t-1). \quad (6)$$

All the measured data  $U_{2n}$  and  $F_n$  are normalized to the range (0,1).

$$U_{2n} = \frac{U_2 - U_{\min}}{U_{\max} - U_{\min}}, \quad F_n = \frac{F}{F_{\max}}. \quad (7)$$

The algorithm of the training set extension is shown in Fig. 5.

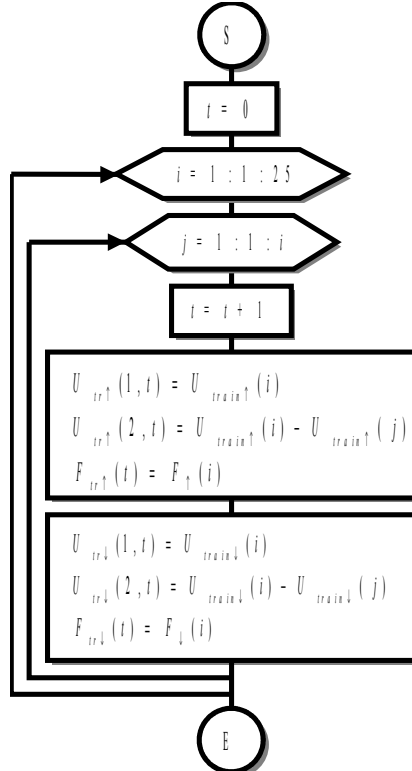


Fig. 5. Algorithm of training set extension.

We have designed two solutions for sensor errors suppression. The first one consists of single feedforward NN - marking as model A (see Fig. 6a) [12]. The second consists of two feedforward NNs (model B, see Fig. 6b), where parameter  $\varsigma$  determines which part of the model will be used (see Fig. 6c). NN1 is activated if  $\varsigma < 0$  and NN2 if  $\varsigma > 0$ . The output of the model is unchanged if  $\varsigma = 0$ . It is described by the next relation:

$$F_{NN}(t) = \begin{cases} \check{sim}(\text{NN1}, (U_2(t), \varsigma(t))) & \text{if } \varsigma(t) < 0 \\ sim(\text{NN2}, (U_2(t), \varsigma(t))) & \text{if } \varsigma(t) > 0 \\ F_{NN}(t-1) & \text{if } \varsigma(t) = 0 \end{cases} \quad (8)$$

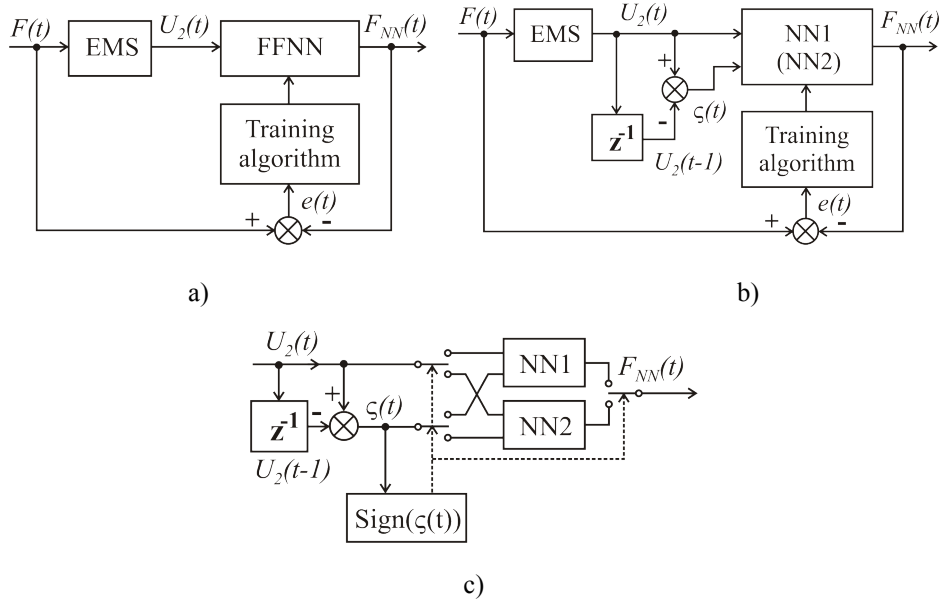


Fig. 6. Proposed models: a) model A - classical FFNN model, b) model B - training of the NN1 (NN2), c) NN selection based on parameter  $\varsigma$ .

The design of the neural network is made in MATLAB7, Neural Network Toolbox 4.0. Function *sim* simulates the network NN1 or NN2 with inputs  $U_2(t)$  and  $\varsigma(t)$ . Partial network NN1 is trained on minor up-loops data and NN2 on minor down-loops data. To obtain the best possible neural network solution we experimented with parameters as the number of epochs, type of training function and number of neurons in the hidden layers. Each layer's weights and biases are initialized with *initnw*. The Levenberg-Marquardt (*trainlm*) training algorithm is used. In general, on function approximation problems, for networks that contain up to a few hundred weights, the *trainlm* algorithm will have the fastest convergence. This advantage is especially noticeable if very accurate training is required. The *trainlm* uses these training parameters:

- performance goal *trainParam.goal* = 0,
- maximum validation failures *trainParam.max\_fail* = 5,
- factor to use for memory/speed trade off *trainParam.mem\_reduc* = 1,
- minimum performance gradient *trainParam.min\_grad* = 1e-10,
- maximum number of epochs to train *trainParam.epochs* = 1000.

The *trainlm* uses an adaptive learning rate. Performance is measured according to the specified network performance function MSE, which returns the mean squared error:

$$\text{MSE} = \frac{1}{N} \prod_{i=1}^N (y_i - t_i)^2, \quad (9)$$

where  $N$  is the number of training data,  $y_i$  is output the vector of neural network ( $F_{NN}$ ),  $t_i$  is the target vector ( $F$ ). The MSE versus training epochs for model A and B are shown in Fig. 7.

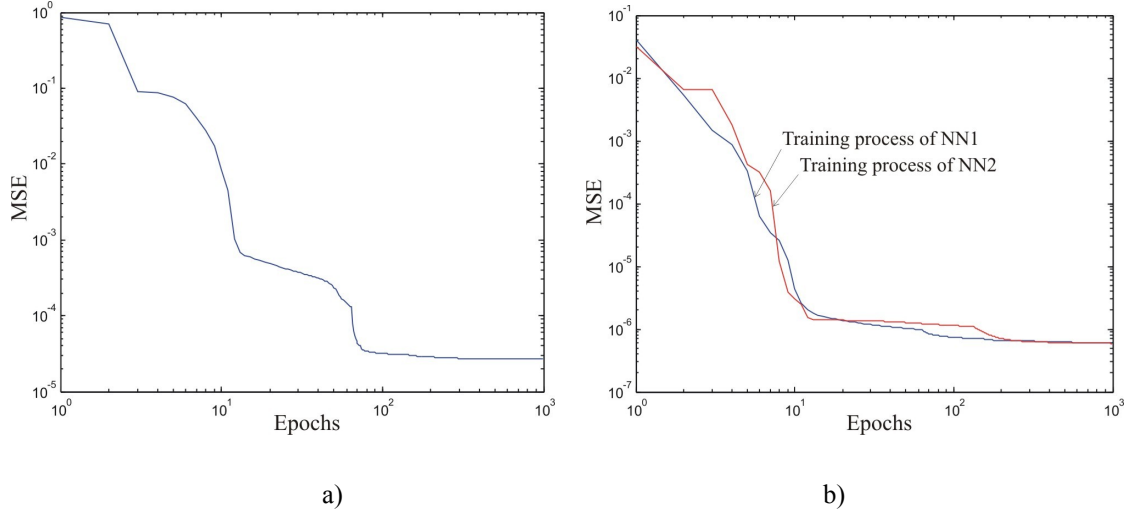


Fig. 7. Training processes of a) model A and b) model B.

Determination of the number of neurons in hidden layers and selection of the network with the best parameters is shown in Fig. 8 (criterion - the smallest hysteresis error) and in Fig. 9 (criterion - the smallest linearity error). NHL1 represents the number of neurons in the first hidden layer (NHL2 - number of neurons in the second hidden layer) in Figs. 8 and 9 (see carefully axis in these figures).

Conclusion - model A is simpler, it has smaller stability. Model B is more stability, however, if it has too many hidden neurons, the network acts like a lookup table.

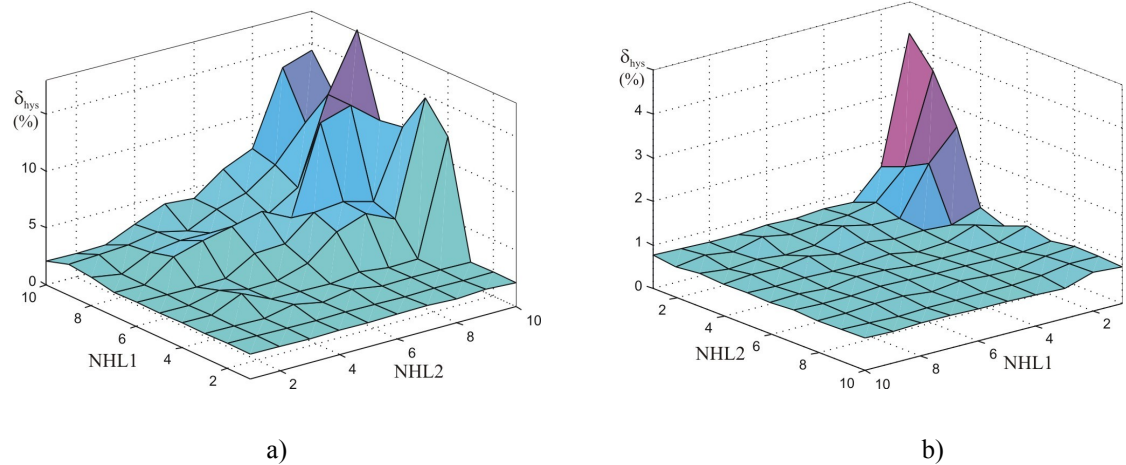


Fig. 8. Hysteresis error of a) model A, b) model B.

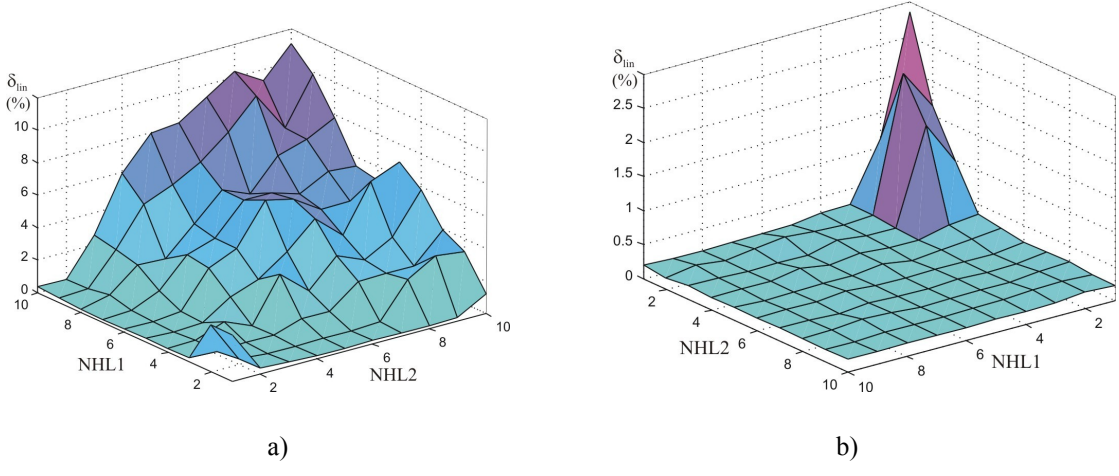


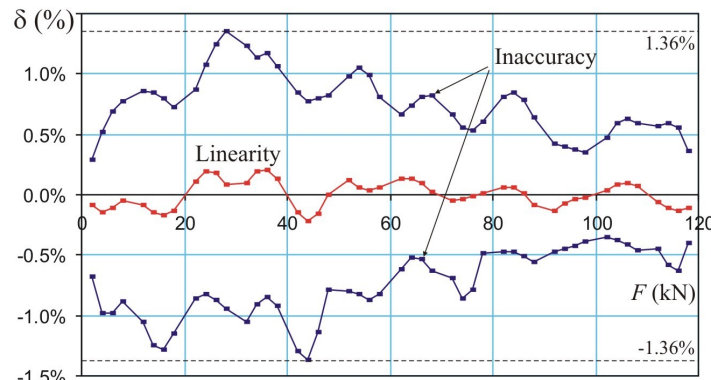
Fig. 9. Linearity error of a) model A, b) model B.

#### 4. EVALUATION OF ERRORS

One of the tasks of neural networks is suppression of linearity and hysteresis errors. From this point of view the network 1-2-3-1 (architecture model A) is better suited for the task than other networks (the network achieves the best task generalization). However, Fig. 8a shows that any of model A cannot suppress the hysteresis error of the sensor. Our proposed architecture model B is much better for errors suppression. With regard to a solution as simple as possible, the network 2-4-5-1 (architecture model B) is chosen for the next evaluation. The Table 2 shows a comparison of the errors suppression for architectures model A and model B with classic approach. Fig. 10 shows the difference between model A and model B error suppression.

Table 2. Comparison of errors.

	classic approach	model A (1-2-3-1)	model B (2-4-5-1)
Inaccuracy	-3.16 %; 5.24 %	-1.36 %; 1.36 %	-0.97 %; 0.75 %
Measured error	4.63 %	1.07 %	0.42 %
Repeatability	1.65 %	1.63 %	1.68 %
Hysteresis	2.13 %	2.04 %	0.57 %
Linearity error	4.63 %	0.22 %	0.19 %



a)

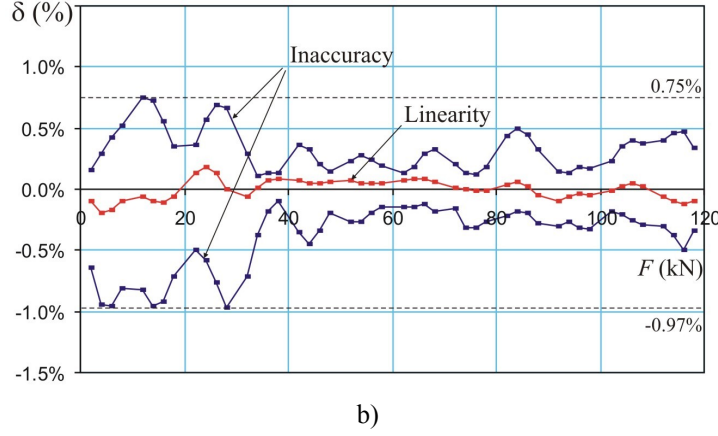


Fig. 10. Comparison of errors - inaccuracy and linearity error, a) model A 1-2-3-1, b) model B 2-4-5-1.

## 5. EVALUATION OF UNCERTAINTIES

Modern measurement theory and practice assume getting a measurement result along with some characteristics of its uncertainty. The uncertainty of the measurement result reflects the lack of exact knowledge of the specified measurand. The ISO Guide [2] defines uncertainty (in Section D.5.2) as an expression of the fact that, for a given measurand and a given result of measurement of it, there is not one value but an infinite number of values dispersed about the result that are consistent with all of the observations and data and one's knowledge of the physical world, and with varying degrees of credibility attributed to the measurand. The Guide assumes that the evaluation of all uncertainty components is based on probability distributions characterised by variances. The variances are either estimated from a series of repeated observations (type A) or assumed to exist and estimated from available knowledge (type B).

The type B evaluation of standard uncertainty is usually based on scientific judgment using all of the relevant information available [6]. The uncertainty of the measurement result  $u_{res}$  consists of three components:

$$u_{res}^2 = u_{ina}^2 + u_{TE}^2 + u_r^2, \quad (10)$$

where  $u_{ina}$  is acquired from sensor inaccuracy,  $u_{TE}$  corresponds with manufacturer's specified accuracy of used force device (test equipment for generating true force  $F$ ) and  $u_r$  is uncertainty of the rounding. In accordance with ISO Guide, rectangular distribution is used if an estimate is made in the form of a maximum range ( $a_-, a_+$ ) with no knowledge of the shape of the distribution. Each component can be expressed by the next equation:

$$u(x) = \frac{a}{\sqrt{3}}. \quad (11)$$

The maximum range ( $a_-, a_+$ ) can be represented by inaccuracy range ( $\delta_{ina-}, \delta_{ina+}$ )/100. Following this knowledge, the next relation can be written:

$$u_{res} = \sqrt{\left( \frac{\frac{c}{2} \frac{\zeta \delta_{ina+} - \delta_{ina-}}{100}}{\sqrt{3}} \right)^2 + \left( \frac{\zeta \delta_{AR}}{100} \cdot MR \right)^2 + \left( \frac{c}{2} \frac{\Delta}{\sqrt{3}} \right)^2}, \quad (12)$$

where  $FS$  is full scale,  $\delta_{AR}$  is accuracy rating of test equipment declared by its manufacturer (generally expressed as a percentage of  $MR$  - measuring range) and  $\Delta$  is rounding (rounded to two significant digits  $\Delta = 0.01$  kN = 10 N). If the distribution of the values is almost symmetrical the influence of rounding on the uncertainty of result is negligible:

$$u_r = \frac{\frac{1}{2} \cdot 10^2}{\sqrt{3}} = 28.87 \text{ (N)} = 0.002887 \text{ (kN)} = 0.00 \text{ (kN)} \quad (13)$$

Computed uncertainties of the measurement result are in Table 3.

Table 3. Uncertainties of the measurement result.

	sensor EMS	model A (1-2-3-1)	model B (2-4-5-1)
$u_{ina}$ (kN)	2.91	0.94	0.60
$u_{TE}$ (kN)	0.12	0.12	0.12
$u_{res}$ (kN)	3.03	1.06	0.71

The result of the measurement is given by:

$$F_{res} = F' \pm u_{res} \text{ (kN)}, \quad (14)$$

where  $F'$  is gained from a measuring system (with or without neural network) and  $u_{res}$  represents the appropriate uncertainty of the system.

## 6. CONCLUSION

The paper brings a new approach to error suppression by using neural networks (model B). It is compared with the common approach of using neural networks (model A) and with the classic approach without neural network. Model B uses a specific extension of the training set based on nonlinear system properties with hysteresis. Moreover, model B uses additional neural network NN2 complementary to NN1 and the parameter  $\zeta$ , which includes the time dimension. Described extension of the training set provides good stability of the network and good independence from the number of hidden neurons (see Figs. 8b and 9b). Implementation of neural networks into the measuring set solves the problem with conversion of output sensor voltage into measured force and suppresses errors; linearity error - from 4.63 % to 0.19 %, hysteresis error - from 2.13 % to 0.57 %.

The second purpose of this paper is to provide a measurement uncertainty analysis of the measuring system with elastomagnetic sensor of pressure force. Significant error sources are identified and quantified and the uncertainty of the measurement result is determined. The presented methodology of error suppression is generally applicable to nonlinear systems with hysteresis. However, the error and uncertainty evaluations are specific to the measurement process and test equipment used.

## ACKNOWLEDGEMENT

The author thanks Dr. Martin Kollár for his help with evaluation of uncertainty. This work has been supported by the Grant Agency of the Slovak Republic VEGA grant No. 1/2180/05.

## REFERENCES

1. Arpaia P., Daponte P., Grimaldi D., Michaeli L.: *ANN-Based Error Reduction for Experimentally Modeled Sensors*. IEEE Trans. on Instrumentation and Measurement, vol. 51, no. 1, 2002, pp. 23-30.
2. Guide to the Expression of Uncertainty in Measurement. BIPM - IEC - ISO - OIML, 1995.
3. IEC 60770, Transmitters for Use in Industrial-process Control Systems - Part 1: Methods for Performance Evaluation, 1999-02, Part 2: Methods for Inspection and Routine Testing, 2003-01.
4. IEC 61298-2, Process Measurement and Control Devices - General Methods and Procedures for Evaluating Performance - Part 2: Tests under Reference Conditions, 1995-07.
5. Jiles D.C., Atherton D.L.: *Theory of Ferromagnetic Hysteresis*. Journal on Magnetism and Magnetic Materials, vol. 61, 1986, pp. 48-60.
6. Kollár M.: *Uncertainty in the System for Measurement of the Capacitances Using Flip-Flop Sensor*. ElectronicsLetters, vol. 4, 2003, www.electronicsletters.com, ISSN 1213-161X.
7. Kováč D.: *Feeding and Evaluating Circuits for an Elastomagnetic Sensor*. Journal of Electrical Engineering, vol. 50, no. 7-8, 1999, pp. 255-256.
8. Kuczmann M., Ivanyi A.: *A New Neural-network-based Scalar Hysteresis Model*. IEEE Transactions on Magnetics, vol. 38, 2002, pp. 857-860.
9. Kvasnica B., Fabo P.: *Highly Precise Noncontact Instrumentation for Magnetic Measurement of Mechanical Stress in Low-Carbon Steel Wires*. Measurement Science and Technology, vol. 7, 1996, pp. 763-767.
10. Mojžiš M., et al.: *Substitute Model and Power Parameters of Elastomagnetic Force Sensor*. Journal of Electrical Engineering, vol. 52, no. 11-12, 2001, pp. 379-382.
11. Panda G., Das D. P., Mishra S. K., Panda S. K., Meher S., Mahapatra K. K.: *Development of an Efficient Intelligent Pressure Sensor Using RBF Based ANN Technique*. International Conference on Intelligent Signal Processing and Robotics, India, Feb 20-23, 2004.
12. Vojtko J., Kováčová I., Madarász L., Kováč D.: *Neural Network for Error Correction of Pressure Force Sensor Based on Elastomagnetic Phenomena*. Proceedings ICCC'2004: 2nd IEEE International Conference on Computational Cybernetics, Vienna University of Technology, Austria, 2004, pp. 143-146. ISBN 3-902463-02-3.

## ZASTOSOWANIE SIECI NEURONOWYCH DO ELIMINACJI BŁĘDÓW W NIELINIOWYCH SYSTEMACH Z HISTEREZĄ

### Streszczenie

Niektórymi z wad nieliniowych systemów z histerezą są stosunkowo duże błędy, np. błąd liniowości, błąd histerezy itp. Artykuł opisuje możliwe ulepszenia metod eliminacji błędów przy zastosowaniu sieci neuronowych. Innym z celów pracy jest oszacowanie niepewności pomiaru. Artykuł dokonuje przeglądu stosowanych obecnie procedur przy obliczeniach niepewności pomiaru zgodnie z Przewodnikiem ISO.